Earthquakes and Structures, *Vol. 23, No. 3 (2022) 315-328*
https://doi.org/10.12989/eas.2022.23.3.315

Machine learning tool to assess the earthquake structural safety of systems designed for wind: In application of noise barriers

Tabish Ali[a], Jehyeong Lee[b] and Robin Eunju Kim*

Department of Civil & Environmental Engineering, Hanyang University, 222, Wangsimni-ro, Seongdong-gu, Seoul 04763, Republic of Korea

(Received June 27, 2022, Revised October 10, 2022, Accepted October 11, 2022)

Abstract. Structures designed for wind have an opposite design approach to those designed for earthquakes. These structures are usually reliable if they are constructed in an area where there is almost no or less severe earthquake. However, as seismic activity is unpredictable and it can occur anytime and anywhere, the seismic safety of structures designed for wind must be assessed. Moreover, the design approaches of wind and earthquake systems are opposite where wind design considers higher stiffness but earthquake designs demand a more flexible structure. For this reason, a novel Machine learning framework is proposed that is used to assess and classify the seismic safety of the structures designed for wind load. Moreover, suitable criteria is defined for the design of wind resistance structures considering seismic behavior. Furthermore, the structural behavior as a result of dynamic interaction between superstructure and substructure during seismic events is also studied. The proposed framework achieved an accuracy of more than 90% for classification and prediction as well, when applied to new structures and unknown ground motions.

Keywords: AI, coupled analysis, ground motions, noise barriers, seismic safety, sensitivity

1. Introduction

Structures designed for wind have an opposite design approach to those designed for earthquakes. Wind designs are stiffer whereas seismic designs are more flexible (Aswegan *et al*. 2017). Thus, the wind design structures are liable to earthquake damage (Chen 2012). Hence, wind resistance structures are designed in regions having low-impact earthquakes or when there is no need to follow the seismic codes (Klingner *et al*. 2003). As such, structures designed for wind are not guaranteed to be safe during an earthquake event and cause severe damage (Ham *et al*. 2005). A lot of studies have been done on the structural safety of systems designed for wind during seismic activity and found that the damage probability is highly sensitive and causes the structural members to yield (Wen *et al*. 2002, Basaran *et al*. 2016, Turkeli *et al*. 2017). Apart from buildings, one of the important non-building structures is a noise barrier (NB) also known as a soundproof wall which is constructed along the roadsides and is used to mitigate noise pollution. Traditionally, the NBs have been designed for wind loads only, where the focus is only on the maximum wind design criteria (Nusairat *et al*. 2004, Kwon *et al*. 2011, Duru 2016, Li 2016, Kim and Jung 2017, Choi and Lee 2018, Sim *et al*. 2018). Some studies also mention the maximum allowable deflection of the NB posts or columns due to wind as a design criteria (Niewiadomski *et al*. 2014, Li 2016). However, like buildings, the earthquakes can cause damage to the noise barrier which results in falling down, tilting and detaching of members (Kazama and Noda 2012, Lin *et al*. 2020a). The literature points the stochastic nature and fatigue effects of wind on NB (Sun *et al*. 2020). Height, shape, and topology optimization studies have also been done (Grubeša *et al*. 2011, Toledo *et al*. 2015, Suhanek *et al*. 2021). Based on the aforementioned studies, design specifications followed by most countries such as AASHTO, EN 14289-2, and manuals of Japan and China are based on the maximum wind velocity and wind load at the location to be constructed (Knauer *et al*. 2000, Klingner *et al*. 2003, Clairbois and Garai 2015). Thus, the earthquake design of NBs is neglected.

Since, its first construction in 1968 in California, United States (U.S.), the global noise barrier market is growing very fast. NB built along highways in the U.S have increased to over 2700 miles in 2010. As the demands on constructing NBs increase, the demands to innovate NB design for better acoustics, strength, and resilience are increasing. The effectiveness of NBs depends on the material, structural design, and mainly the height of the NB (Simpson 1976, Knauer *et al*. 2000, Klingner *et al*. 2003). Moreover, with the development of cities, the construction of NBs is increasing in both length and height and the concept of tall NBs is emerging (Bose 2010, City and Assessment 2010). Despite their enhanced acoustic capabilities, tall NBs can cause some structural instability. The tall NBs, over 20 m in height, may have significantly low resonance frequency and are liable to resonate with the

*Corresponding author, Assistant Professor
E-mail: robinekim@hanyang.ac.kr
[a]Ph.D. Student
E-mail: taoab386@hanyang.ac.kr
[a]Master's Student
E-mail: lk1696@naver.com

ISSN: 2092-7614 (Print), 2092-7622 (Online)

low-frequency vibrations arising from large vehicles, wind, and low-frequency earthquakes. To compensate for the effect of the earthquake (EQ), some design guides provide EQ design accounting for the equivalent lateral force procedure (ELFP) (Wassef *et al*. 2010). However, the safety criterion is left on the engineer's intuition (Chen and Cai 2004). The effects of the low-frequency feature of tall NBs on their dynamic responses subject to vehicle vibration and EQs have been explored by few researchers. Tokunaga *et al*. (2013) developed a simplified single degree of freedom (SDOF) model and a 2-DOF model for NBs on a railroad bridge to examine the effect of resonance behavior. The study has found that the impact of EQ cannot be neglected for NBs whose natural frequencies are 5Hz or less. Then the research group investigated the interaction dynamics between the NB and the bridges subject to vehicle passage for a railroad bridge (Tokunaga *et al*. 2016b, Tokunaga *et al*. 2016a). Using sophisticated finite element models, (Zheng *et al*. 2020) evaluated the acceleration response of the NBs on a railroad bridge subject to high-speed vehicles. The responses are examined to compare several design alternatives and distinguish a component vulnerable to EQs. The aforementioned studies well emphasized that the interaction dynamics of the tall NBs with vibration sources cannot be neglected. However, only a limited number of design EQs are selected and the engineering demand parameters (EDPs) that consists of acceleration, drift, and base shear (Kim and Roschke 2006, Xu *et al*. 2017) have not been fully investigated. Therefore, in-depth understanding on dynamic interaction responses of NBs with bridges subjected to wide range of EQs deserves to be made.

The use of computer applications are on a rise in structural engineering, especially earthquake engineering (Deng *et al*. 2005, Falcone *et al*. 2020, Li *et al*. 2020). Performance-based seismic design (PBSD) has a huge demand of computation, thus, computer-aided design is a necessity in seismic and structural engineering (Pan and Dias 2017, Lee and Jeong 2018, Salehi and Burgueño 2018). For example, the analysis period increases exponentially with the model complexity in PBSD (Salgado and Guner 2018). Kappos and Panagopoulos (2004) found significant computational time for the PBSD of a simple 3D building using the well-known software SAP2000. Huge computational demand using finite element analysis to solve multiple degrees of freedom systems with the increase in matrix's size is pointed out by (Nguyen 2006). Among various Machine Learning (ML) technologies, classifier-based learning and neural techniques regression-based learning are adopted in various EQ applications. A classifier-based learning is used to classify the buildings based on structural damage, failure mode and structural performance (Mangalathu and Jeon 2018, LEÓN *et al*. 2019). Whereas other groups of researchers used Artificial Neural Networks (ANN) and Support Vector Machines (SVM), which can dramatically reduce the computational cost, in predicting the seismic response of structures (Lagaros and Papadrakakis 2012, Farfani *et al*. 2015, Mirhosseini 2017, Moeindarbari and Taghikhany 2018, Lin *et al*. 2020b, Oh *et al*. 2020, Sainct *et al*. 2020). So far both approaches have been widely adopted in applications such as structural safety assessment, damage classification, crack detection, soil structure interaction (SSI), soil pile structure interactions (SPSI) and seismic fragility curves (Abdel-Qader *et al*. 2006, Li *et al*. 2016, Amiri and Rajabi 2018). Regarding application of ML in NBs, only few researches have been found, especially focusing on the optimization of the heights and noise attenuation parameters considering the acoustic characteristics, environmental effects, and traffic flow (Zannin *et al*. 2018, Dhiman *et al*. 2021). Thus, assessing the design criteria of NBs based on predicted responses using ML needs more detailed studies.

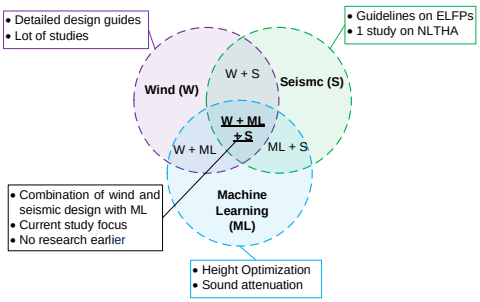

Fig. 1 Studies related to Noise Barrier Design

Consideration of seismic safety assessment of wind-designed structures is becoming unavoidable for ensuring the resilience of the structures, as discussed in the above paragraphs. Thus, a computer-aided advanced framework is proposed for NBs on bridges to overcome the mentioned safety concerns. The proposed framework aims to solve the nonlinear time history analysis (NLTHA) of tall NBs and bridge structures considering their dynamic interaction (coupled behavior). It first determines whether a wind design is sufficient, or a seismic design is required by assessing the design parameters. In the categorization of the results, optimized Ensemble, a classification-based learning algorithm is utilized. Once classified as a seismic design, the framework further divides the structure into coupled and uncoupled models based on the dynamic interaction of the bridge and NB which will be further discussed in the upcoming paragraphs. The seismic responses of those systems are predicted from a proposed ANN model. Note that the Ensemble-based classification achieves about 93 % accuracy and ANN can predict the responses with an accuracy above 90 %. Thus, the presented framework can help the designers in choosing wind or earthquake design, coupled or uncoupled design and getting the seismic response of NBs with less computation and more accuracy. Therefore, the main objective of the paper is to stress the importance of seismic structural safety of systems designed for wind. The authors have contributed to the scientific knowledge by using machine learning to assess the design of NB structures classifying them into the wind and seismic models and pointing out the importance of dynamic interaction of structures with a classification of coupled and uncoupled models as per the seismic demands. Lastly, using the proposed framework, the seismic responses of the structures are accurately predicted. The area and contribution of this research are shown in Fig. 1 as a Venn diagram. The detailed results of the study are discussed in this paper.

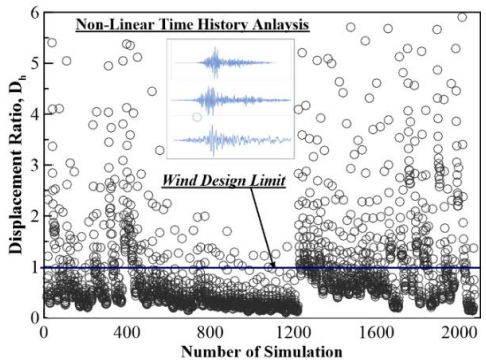

Fig. 2 Wind design limit

2. Assessment of seismic safety of structures designed for wind

Fig. 2 shows 2000 simulation results of NLTHA to illustrate that the wind design of a NB is insufficient for some cases thus requiring a seismic design. It shows the upper limit of wind design criteria based on the deflection value of the NB discussed in detail in section 3. It is also worth mentioning that a coupled analysis is required for some earthquakes and not for others depending on the characteristics of the ground motion. These issues are validated against multiple earthquakes from China, Japan, and Taiwan. Fig. 3 (a), (b) and (c) show the responses obtained using Taiwan EQ responses in the form of a ratio of maximum acceleration (K_h), maximum displacement (D_h), and maximum base shear (V_h) of the structure (also discussed in section 3) emphasizing the importance of interaction. It can be noted that for some cases the uncoupled behavior is conservative while coupled behavior is necessary in general cases. Thus, the proposed methodology differentiates such cases to ease the designer ensuring safety and economy and fulfills these necessities with the help of an advanced machine learning framework.

3. Computer-aided framework

The proposed next generation computer-aided framework has three primary parts as shown in Fig. 4. These are database creation, machine learning-based design type selection, and artificial neural network-based seismic response prediction. The input parameters are related to earthquake, structure, and interaction between super-structure and sub-structure (interaction between structures) and soil while the outputs are related to the design assessment like wind or seismic design, coupled or

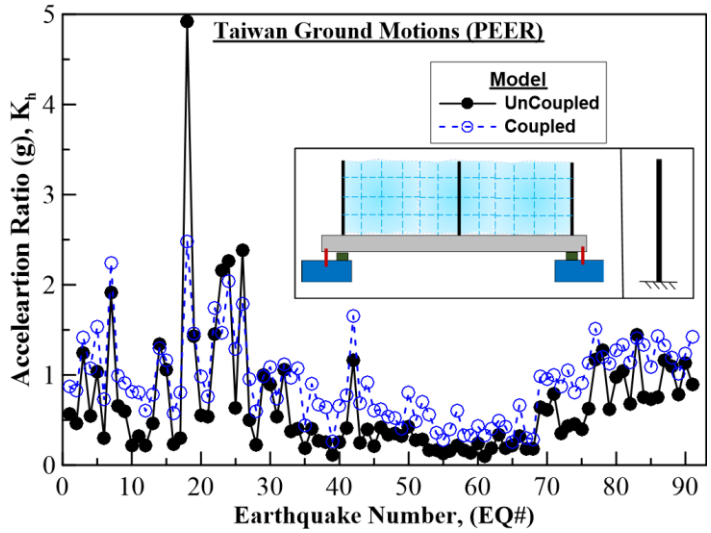

(a) Coupled vs. uncoupled acceleration response

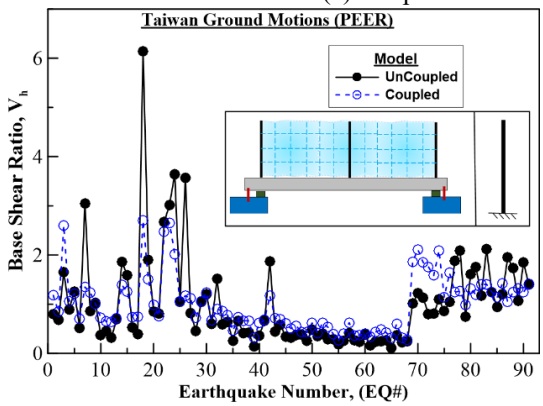

(b) Coupled vs. uncoupled base shear response

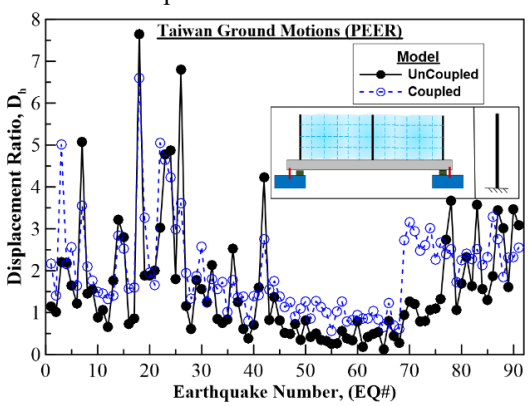

(c) Coupled vs. uncoupled displacement response

Fig. 3 Comparison of coupled and uncoupled behavior of NBs during Earthquake

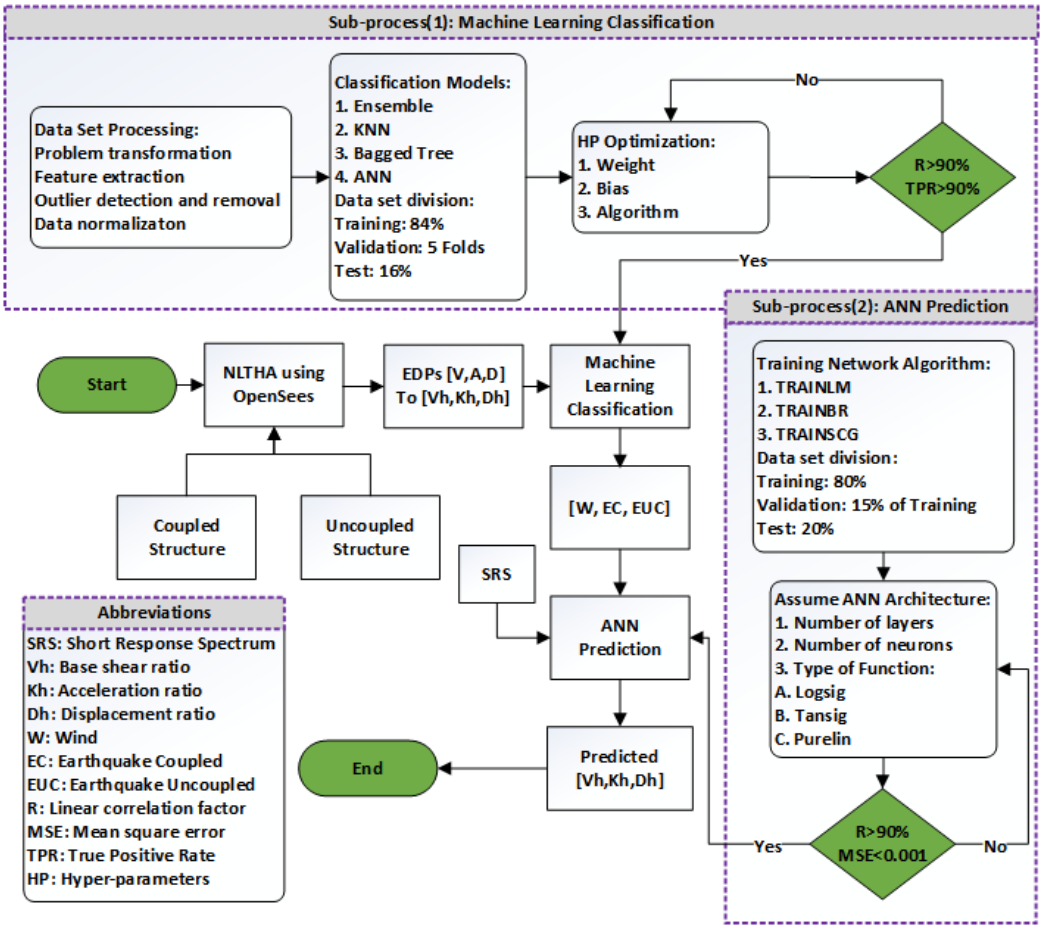

Fig. 4 Flow chart of the framework

uncoupled design and response of structure (K_h), (D_h), (V_h) for the performance evaluation.

3.1 Methodology

A finite element-based software OpenSees (McKenna 2011, OpenSees 2011) is used to create preliminary models and a resulting database that further be applied for AI techniques embedded in MATLAB R2021a (MATLAB 2021). Firstly, the framework gives the design type i.e., whether a seismic design is needed, or the conventional wind design is sufficient. Secondly, for seismic design type, the framework gives the design category i.e., whether one should consider the dynamic interaction or not. These decisions are based on A_c, which is a structural design assessment ratio, obtained as follows

$$A_c = W + S \tag{1}$$

where W is the wind design indicator and S is an interaction indicator, which checks the design guides. First, based on the response of the model, displacement ratio (D_h) is calculated from the ratio between the maximum displacement (D) subjected to EQ and the displacement limit (D_1) from the wind design.

$$D_h = \frac{D}{D_1} \tag{2}$$

Note that based on the construction condition of the NB, D_1 is taken as below in this study (Li 2016, 2018)

$$D_1 \leq \frac{H}{125} \text{ , for NBs on ground} \tag{3}$$

or

$$D_1 \leq \frac{H}{300} \text{ , for NBs on a bridge} \tag{4}$$

If $D_h < 1$ then, W = 0 and S (interaction indicator) = 0. These values imply that the displacement by EQ is not exceeding wind design limits, assuring that the conventional wind design is sufficient. On the other hand, if $D_h \geq 1$ then, W=1 and further assessment is required to check S.

S is also a Boolean (i.e., taken either 1 or 0), based on S_h (design category ratio) calculated from the equation below

$$S_h = \frac{D_c}{D_{uc}} \tag{5}$$

here, D_c and D_{uc} are the maximum displacement from a Coupled model and an Uncouple model, respectively, obtained from NLTHA. A detailed explanation of the NLTHA process will be discussed in Section 3. If the design category ratio, $S_h < 1$ then, S=0. Section 4 a setting indicates that using an uncoupled EQ design, which is simpler than coupled design, is sufficient. On the other hand, if $S_h \geq 1$ then, take S=1 which means coupled EQ

Table 1 Database distribution for ML and ANN training and testing

	ML Classification	ANN Prediction
Total Dataset	3557	7114
Train	3000	5714
Validation	5 folds valid.	857
Test	557	1400

design is required.

In summary, the structure design assessment ratio is as follows:

If $A_c = 0$, then go for wind design (W).

If $A_c = 1$, then go for earthquake uncoupled design (EUC).

If $A_c = 2$, then go for earthquake coupled design (EC).

Lastly, the framework predicts the seismic responses (K_h, D_h, V_h) for performance evaluation. To get the best results, different ML and ANN techniques are performed by updating various hyper-parameters. The ANN model is simulated for both multi input single output and multi input multi output systems to select the better one based on the overall accuracy.

3.2 Base model and database creation

The dataset is created from a base model representing a real-life traffic noise barrier (Soundproof wall) system which is under construction in South Korea. This base model is also compared in terms of frequencies and seismic coefficient responses using the same earthquakes as mentioned in a previous real-life structure from Japan (Tokunaga *et al*. 2013, Tokunaga *et al*. 2016b) to avoid any inconsistencies before creating the database. The results were in the acceptable error range of 10%. Then the database is constructed containing input parameters such as the height of the structure (H), the design category of structure (S), based on the seismic interaction of the structures, the peak ground acceleration (PGA), short response spectrum (SRS), shear wave velocity of the earthquakes (V_s), and the ground type (G) as well. Output parameters included dimensionless EDPs: acceleration in terms of gravity (K_h), displacement ratio (D_h) and base shear from NLTHA divided by ELFPs base shear (V_h). To improve the AI techniques, data processing, such as removal of outliers and normalization of the original data has been performed. The following formula is used to normalize the data

$$x_n = \frac{x - x_{\min}}{x_{\max} - x_{\min}} \tag{6}$$

where x_{n} is the normalized value, x is the input value, $x_{\min}$ and $x_{\max}$ are the minimum and maximum values of x.

The two sets of the database are prepared: One for the ML classification and the other for ANN prediction. The characteristics of the database are shown in Table 1. The training data consists of 84% with 5 folds for cross-validation and the test data is 16% of the total database for ML classification. Whereas the data is divided into 80% and 20% for ANN prediction. To avoid over-fitting, 15% of training data is used for validation during training.

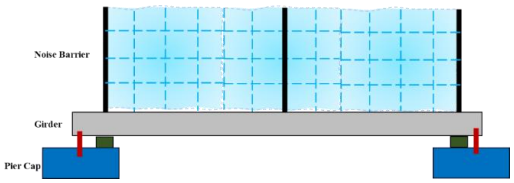

Fig. 5 The Noise Barrier System

Table 2 The geometrical and material properties of the system

Parameter (symbol)	Pier/ Column	Girder/ Beam	NB Post
Elastic Modulus (E)	286 GPa	286 GPa	200 GPa
2nd Moment of Area (I_z)	2.41×10^{11} mm^4	2.41×10^{11} mm^4	6.54×10^{8} mm^4
Weight (W)	230 kN/m	230 kN/m	1023 kN/m
Height (H)	5.605 m	-	18 m

4. Modeling

As stated earlier, OpenSees is used to simulate the system. In this part, two important aspects are discussed: The description of the FE model for the NB and the selection of earthquakes.

4.1 Noise barrier structure

Due to the increasing number of high-rise apartments and buildings, tall NBs along the roadside are emerging in South Korea. One of the newly proposed designs is selected for analysis in this study where the NB height reaches about 18 m, far beyond the conventional designs. A typical NB is shown in Fig. 5. Two types of models are considered for this study, one is the simple or uncoupled NB structure and the other is the sophisticated or coupled NB structure considering the interaction with the bridge where it is constructed. The post of NB is made up of steel, the beam/ girder is constituted of plain concrete and columns/ piers of the bridge are made up of reinforced concrete. In OpenSees, the post is created using elastic BeamColumn element with distributed mass, the girder is also created using the same element with a lumped mass option, whereas the pier is created using nonlinear BeamColumn element with 5 integration points for the fiber section to include the eight steel reinforcement bars. The materials used for concrete and steel are Concrete01 and Steel01 respectively. The compressive strength (f_c') of steel is used as 0.06 kN/mm^2 and the yield strength (F_y) of steel bars is used as 0.46 kN/mm^2. The steel damping ratio is considered 2% and the concrete damping ratio is taken as 5%. The material and geometric properties of the structure are summarized in Table 2. As far as the design is concerned, wind design is sufficient for some cases and others require seismic design. In the same manner, a coupled analysis is required for some earthquakes and not for others depending on the characteristics of the ground motion. These points have

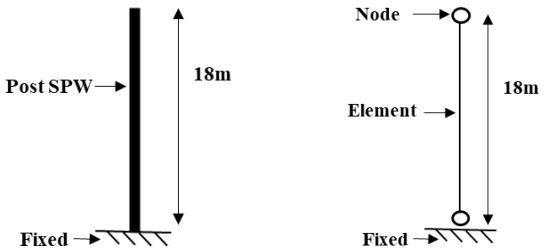

Fig. 6 Uncoupled Noise Barrier Model

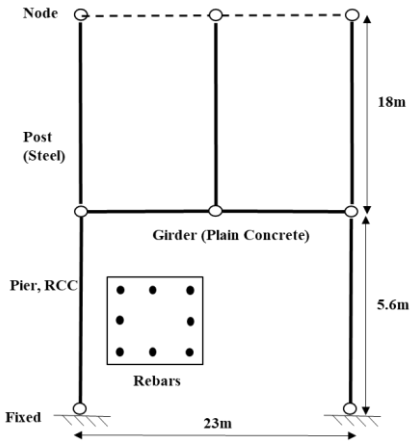

Fig. 7 Coupled Noise Barrier Model

already been stated in the introduction and are further illustrated in section 5.

As shown in Fig. 6, the uncoupled model consists of the NB part only ignoring the bridge on which it is located. It consists of the pole representing the NB with the bottom part restrained in all degrees of freedom and free at the top. The fundamental frequency of the uncoupled base model is about 1.67 Hz.

The coupled model as shown in Fig. 7 is more sophisticated and considers the bridge on which the NB is mounted. It also takes into account the dynamic interaction between these two structures as the NB and bridge are coupled to the same nodes. The fundamental frequency of the coupled base model is about 0.83 Hz.

4.2 Ground motions

Even though South Korea is not in a high seismic zone, but seismologists have warned that a bigger earthquake might come due to the series of recent small tremors (Ryall 2020). This statement is also true because its neighboring regions like Japan, China, and Taiwan are seismically very active. Keeping this in mind, about 200 representative real-life ground motions, obtained from PEER database (PEER) for these 3 regions have been used in this study. In other words, the structure is assumed to be in these three regions. To apply the ground motions, response spectrum (frequency contents) and PGA, that represent dominant non-linear characteristics of the earthquakes are considered (Kim *et al*. 2019, Oh *et al*. 2020). To represent the soil type conveniently, the shear velocity of the ground motion excitations is also included. The database has a variety of parameters for the EQs including the PGA, magnitude (Mw), source-fault mechanism, site to source distance, shear velocity (Vs_{30}), and lowest usable frequency. Representative ground motion characteristics are presented in Table 3 and the peak response spectra are shown in Fig. 8.

5. Application of artificial intelligence

Two types of AI techniques are used in this study. Firstly, Machine Learning Classification is used to classify the structures into three types which are W, EUC, and EC as discussed earlier. Secondly, ANN is used to predict the seismic responses of the structures. For ANN, both Multi Input Single Output (MISO) and Multi Input Multi Output (MIMO) systems are considered. Lastly, a sensitivity analysis is also performed to point out important parameters.

5.1 Machine learning classification

In this section, different classification techniques are applied using built-in tools in MATLAB to select the most

Table 3 Characteristics of some ground motions used in the study

	EQ Name (PEER Sequence #)	PGA (g)	Magnitude (M_w)	Source to Site distance (km)	V_s30 (m/s)	Lowest useable frequency (Hz)	Source-Fault Mechanism
Ground Motion samples	Chi-Chi Taiwan 1180	0.1374	7.62	24.96	235.13	0.0375	Reverse Oblique
	Taiwan SMART1 504	0.2058	6.32	55.96	308.39	0.1250	Reverse
	Taiwan SMART1 492	0.0642	5.80	41.24	314.33	0.2875	Normal
	Chi-Chi Taiwan 1197	0.6364	7.62	3.12	542.61	0.1500	Reverse Oblique
	Kobe Japan 1100	0.2206	6.90	24.85	256	0.0250	Strike-Slip
	Kobe Japan 1107	0.2403	6.90	22.50	312	0.1250	Strike-Slip
	Tottori Japan 3873	0.0693	6.61	115.23	670.13	0.0413	Strike-Slip
	Tottori Japan 3947	0.7323	6.61	5.83	446.34	0.0625	Strike-Slip
	Kobe 1120	0.6177	6.90	1.46	256	0.1250	Strike-Slip
	Northwest China 1755	0.1350	5.80	35.60	341.56	0.3000	Normal Oblique
	Northwest China 1752	0.3001	6.10	9.98	240.09	0.4000	Normal
	Northwest China 1749	0.0354	5.90	12.62	240.09	0.4000	Strike-Slip

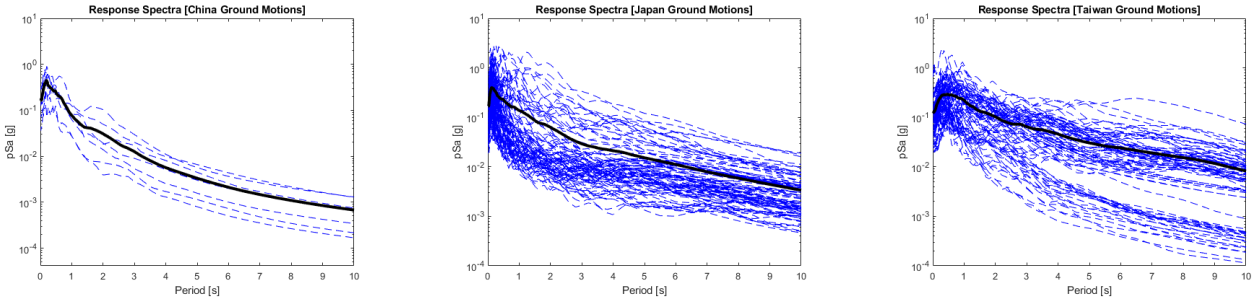

(a) China input EQs (b) Japan input EQs (c) Taiwan input EQs

Fig. 8 Peak response spectra of ground motions from PEER database

Table 4 Architecture of ML techniques

Properties	Ensemble 1	Ensemble 2	KNN
Method	RUS Boost	Bag	Weighted
Splits max.	531	2999	-
Learners/ Neighbors	276	30	10
Learning Rate/ Type	0.01983	Decision Tree	Square inverses

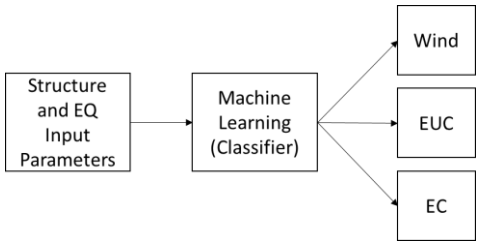

Fig. 9 Overview of the classification framework

suitable method. Around 150 different modules are made by updating the heuristic functions and hyperparameters of different techniques: SVM is a binary linear classifier (Cortes and Vapnik 1995), Ensemble uses an algorithm to learn a group of classification data at the same time and then evaluates them (Bramer 2013), K-nearest neighbors (KNNs) work on the principle of feature similarity avoiding assumptions, and Neural Network that simulates the human brain to predict the output (Kiani *et al*. 2019) etc. Among various, three models Ensemble 1 (RUS-Boost), Ensemble 2 (Bag), and KNN (City-block) are finalized, which showed the highest accuracy for both training and testing. The processing time is about 13s, 3.15s and 2.54s respectively. The weights of these modules are selected such that they give the most conservative results thus, the design would always be on the safe side. The characteristics are shown in Table 4. The input consists of 6 features excluding the SRS and S while including 2 acceleration ratio terms K_{hc} and K_{huc} representing the accelerations obtained from both coupled and uncoupled models. The idea is illustrated in Fig. 9.

As discussed earlier 3 ML techniques were compared and Ensemble 1 (RUS-Boost) is selected for the proposed framework as it outperformed all other techniques in terms of accuracy as shown in Table 5, true positive rate (TPR) and false negative rate (FNR). Fig. 10 shows the TPR and FNR values for Ensemble 1.

5.2 Artificial Neural Network (ANN) prediction

Table 5 Train and test accuracy of ML models

Accuracy	Ensemble 1	Ensemble 2	KNN
Train/ Validation	93.5 %	93.4%	92.9%
Test	93.4%	93.2%	87.3%

ANN is one of the powerful techniques for prediction. The ANNs are trained using Feed-forward backpropagation, a technique where the error is reversed engineered to update the weights and biases of the hidden layers (Rajput and Verma 2014), with the different number of neurons, hidden layers (1, 2, 3, 4), training functions like Levenberg-Marquardt (TRAINLM) is a good technique for medium-sized databases (Singh *et al*. 2005), Bayesian Regularization (TARINBR) algorithm is based on the Bayesian statistics (Gep and Tiao 1973). This method is introduced by MacKay and Neal, and it gives a probability distribution over the predicted values (Neal 1992), TRAINSCG: Scaled Conjugate Gradient works well for big-sized databases (Fletcher 2013) and transfer functions like Tangent Sigmoid (TANSIG), Pure Linear (PURELIN) and LOG-Sigmoid (LOGSIG) that uses the inputs from a layer to calculate the outputs (MathWorks 2005), available in MATLAB. The number of neurons is selected according to Table 6 (Sonmez *et al*. 2006). The judging (selection) criteria for the best ANN model is based on Mean squared error (MSE) and liner correlation (R) coefficient. The inputs are 11 parameters as discussed earlier whereas the outputs are divided into single and multiple vectors. To propose an efficient architecture of ANN, networks with different numbers of output (i.e., MISO and MIMO system) are compared. To evaluate the performance, the normalized MSE and R values are calculated as follows (Farfani *et al*. 2015)

$$MSE = \frac{I \times J \times \frac{1}{I}\left[\sum_{i=1}^{I}\sum_{j=1}^{J}(t_{ij} - y_{ij})^{2}\right]}{\sum_{j=1}^{J}\frac{I\sum_{i=1}^{I}t_{ij}^{2} - (\sum_{i=1}^{I}t_{ij})^{2}}{I}} \tag{7}$$

$$R = \frac{\frac{(\sum_{i=1}^{I}(t_i - \hat{t})(y_i - \hat{y}))}{I}}{\sqrt{\frac{\sum_{i=1}^{I}(t_i - \hat{t}_i)^2}{I}} \times \sqrt{\frac{\sum_{i=1}^{I}(y_i - \hat{y}_i)^2}{I}}} \tag{8}$$

Where I represents the number of test set, J stands for the number of output layer's neuron, t_{ij} and y_{ij} are the predicted and actual solutions for the i^{th} series of the data

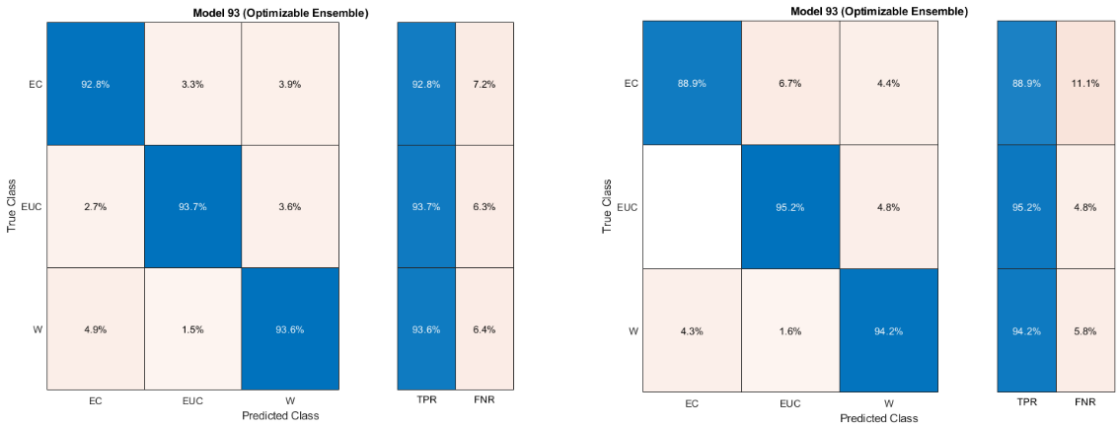

(a) Training data (b) Test data

Fig. 10 True positive rate and false negative rate percentage (Ensemble 1)

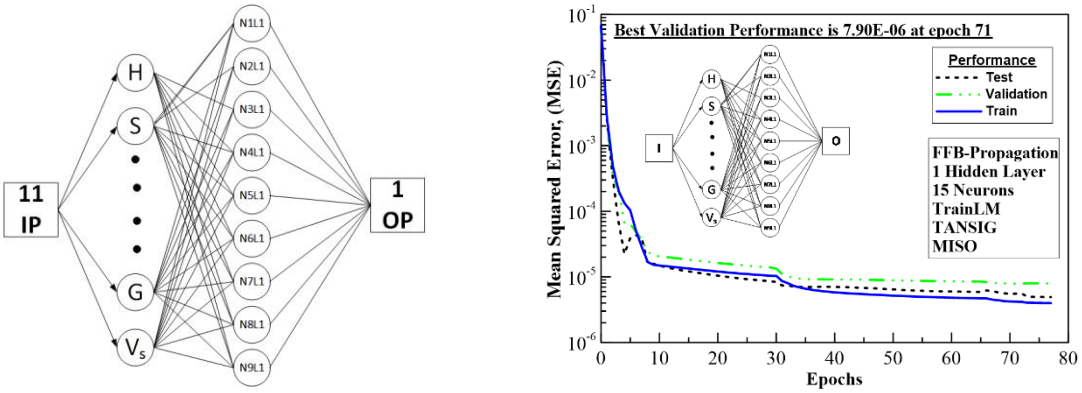

(a) MISO ANN architecture (b) Performance curve of D_h

Fig. 11 ANN architecture and performance of MIMO model

Table 6 Calculation of neurons in the hidden layer

Serial Number #	Heuristic Function	Number of Neurons (Nodes)
1	$\leq 2 \times N_i + 1$	23
2	$3 \times N_i$	33
3	$\frac{2 + (N_o \times N_i) + (0.5 \times N_o) \times (N_o^2 + N_i) - 3}{N_i + N_o}$	For N_o =1 (MISO), 1 For N_o=3 (MIMO), 4
4	$(2 \times N_i) \div 3$	7
5	$2 \times N_i$	22
6	$(N_i + N_o) \div 2$	For N_o =1 (MISO), 6 For N_o=3 (MIMO), 7
7	$\sqrt{(N_i + N_o)}$	For N_o =1 (MISO), 3 For N_o=3 (MIMO), 4

*N_i is the number of input neurons, N_o is the number of output neurons.

given j^{th} node of the output layer. $\hat{t}, \hat{y}$ are the means of these solutions, t_i and y_i are the predicted and actual solutions for the i^{th} series of the set.

The ANN network is transformed into a mathematical formula as below (Das 2013)

$$Y = f_{sig}\left\{b_o + \sum_{k=1}^{h}\left|W_k \times f_{sig}\left(b_{hk} + \sum_{i=1}^{m} W_{ik}X_i\right)\right|\right\} \quad (9)$$

where Y is the normalized output, f_{sig} is the transfer function, b_o is the bias of the output layer, W_k is the connection weight between the k^{th} node of the hidden layer and the single output node, b_{hk} is the bias of the k^{th} node of the hidden layer, h is the number of nodes in the hidden layer, W_{ik} is the connection weight between the i^{th} input variable and the hidden layer and X_i is the normalized output.

5.2.1 Multi input single output ANN model

In MISO scheme, ANNs are tested for each output parameter (D_h, K_h, V_h) separately. The architecture is shown in Fig. 11(a). However, the same number of neurons (15 perceptrons) presented the maximum accuracy for each of the response parameters. Fig. 11(b) shows the performance of D_h in terms of MSE which is 7.9E-6 as compared to K_h

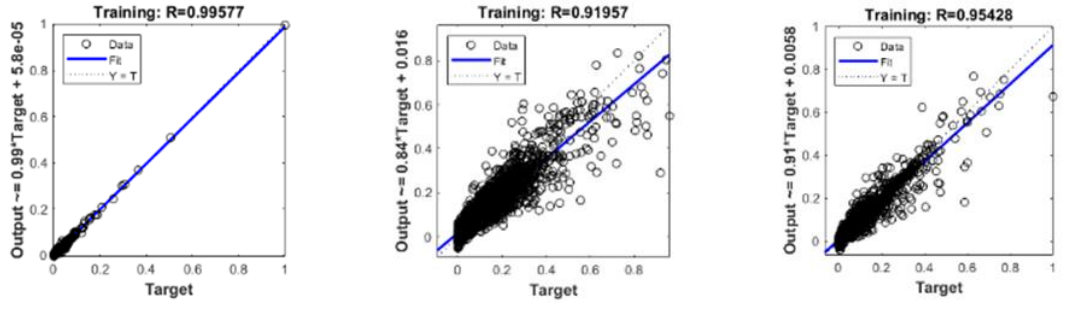

(a) Training R for D_h (b) Training R for K_h (c) Training R for V_h

(d) Validation R for D_h (e) Validation R for K_h (f) Validation R for V_h

Fig. 12 Training and validation linear correlation factor (R) values

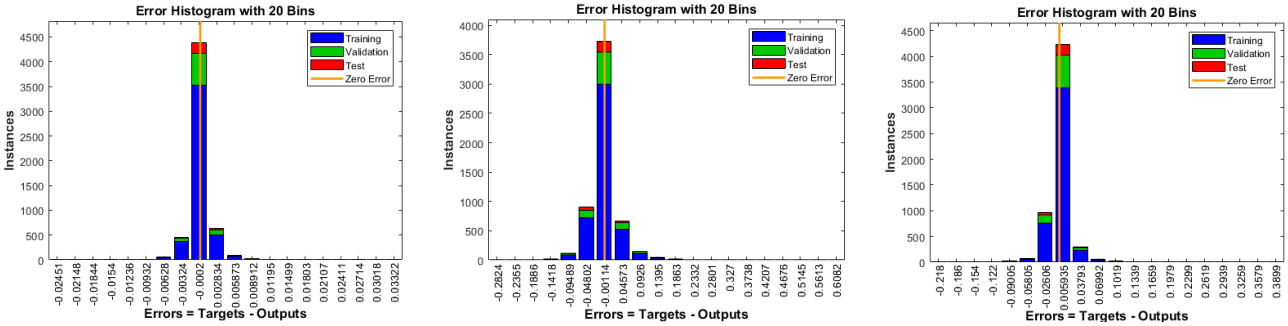

(a) D_h Error Histogram (b) K_h Error Histogram (c) V_h Error Histogram

Fig. 13 Error histograms for training, validation and test linear correlation factor (R) values

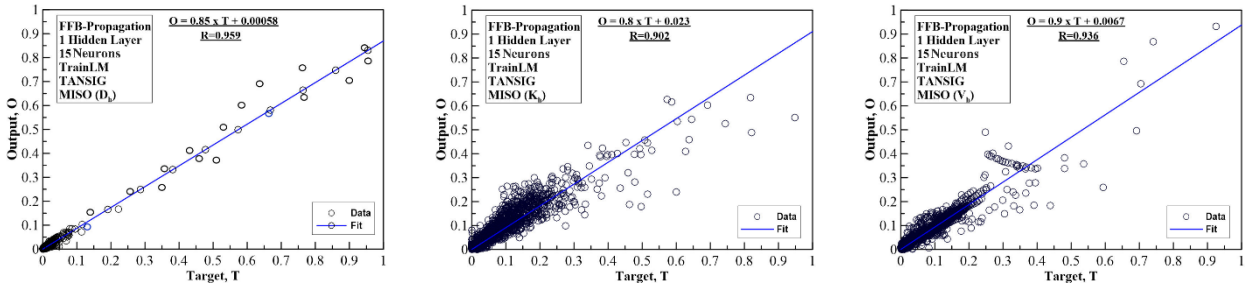

(a) Test R vlaue fo D_h (b) Test R vlaue fo K_h (c) Test R vlaue fo V_h

Fig. 14 Multiple input single output model test linear correlation factor (R) values

and V_h having MSE values of 0.0002 and 0.0006 respectively. The training and validation R values are shown in Fig. 12. The error histograms are presented in Fig. 13. The test on new data is shown in Fig. 14. It can be seen that the training accuracy of D_h is more than the other two parameters in terms of R, being 0.99, 0.91 and 0.95 for D_h, K_h and V_h respectively. D_h is the most important parameter in our framework as the classification is done based on it as discussed in section 2.1.

5.2.2 Multi Input Multiple Output (MIMO) ANN model

In MIMO scheme, the ANNs are tested for a combined output with the 3 parameters (D_h, K_h, V_h). In the case of the MIMO model 25 neurons in the hidden layer provided acceptable results as shown in Fig. 15. The R-value is shown in Fig. 16 along with the error histogram. The test on

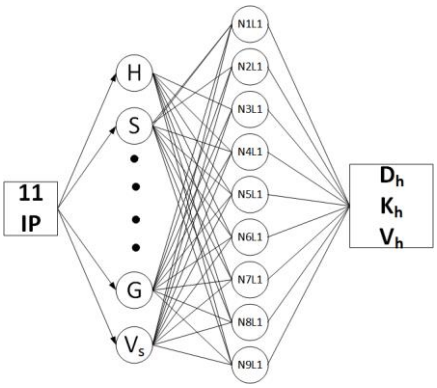

(a) MIMO ANN architecture

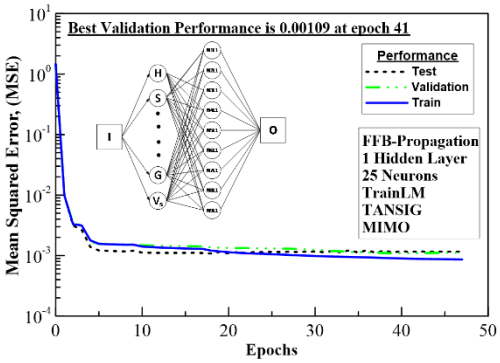

(b) MIMO performance curve

Fig. 15 ANN architecture and performance of MIMO model

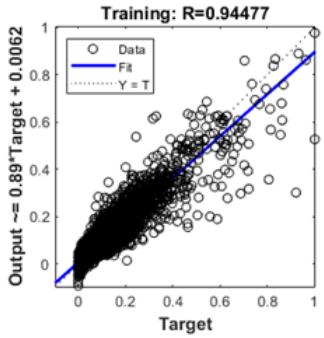

(a) Training *R*

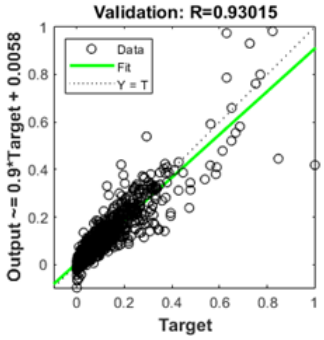

(b) Validation *R*

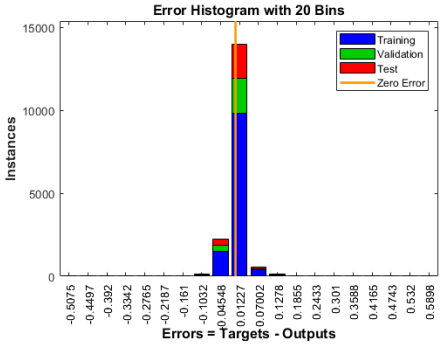

(c) Error Histogram

Fig. 16 Training, validation R values and error histogram of multiple input multiple output model

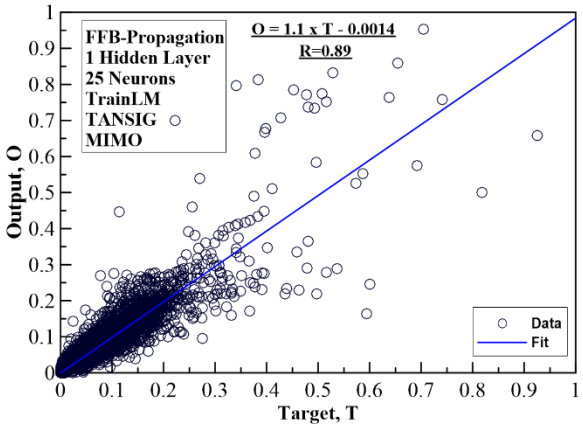

Fig. 17 MIMO test *R*-value for combined (D_h, K_h, V_h)

new data is shown in Fig. 17. The overall performance and accuracy of training and test for MIMO is less than the individual MISO models. The training MSE and R values for MISO is 7.9E-6 (D_h) and 0.99 (D_h), whereas those for MIMO model are 0.001 and 0.94 respectively.

The results from MISO and MIMO are summarized in Table 7 to better compare the results. Overall test accuracy of MISO is showing better accuracy than MIMO model. The best results are obtained with feed-forward back-propagation algorithm using TRAINLM as training function and TANSIG as transfer function. It can also be seen that D_h is predicted with the most accuracy as compared to K_h and V_h.

Table 7 Comparison of MISO and MIMO Models

Model	MISO			MIMO
Parameters	D_h	K_h	V_h	(D_h, K_h, V_h)
Test R	95%	90%	93%	89%
MSE	7.91e-6	0.00274	0.000640	0.0010
Training Time (seconds)	0	0	0	1

5.2.3 Sensitivity analysis

Sensitivity analysis to figure out the most important inputs is performed according to Garson's algorithm using the formula mentioned below (Garson 1991, Gevrey *et al.* 2003). The results are shown in Table 8. Seismic responses are the most sensitive to SRS. Then the dynamic interaction (S) is effective. The height (H) has more relative importance (RI) as compared to ground type (G) and shear wave velocity (Vs).

$$I_j = \frac{\sum_{m=1}^{m=Nh}\left(\left(\frac{|W_{jm}^{ih}|}{\sum_{k=1}^{k=Ni}|W_{km}^{ih}|}\right)\times|W_{mn}^{ho}|\right)}{\sum_{k=1}^{k=Ni}\left\{\sum_{m=1}^{m=Nh}\left(\frac{|W_{km}^{ih}|}{\sum_{k=1}^{Ni}|W_{km}^{ih}|}\right)\times|W_{mn}^{ho}|\right\}} \quad (10)$$

Here, I_j is the relative importance of the j^{th} input on the output. Subscripts k, m and n refer to input, hidden and output nodes, respectively. N_i and N_h are the number of input and hidden nodes, and W is the weight of connection (Elmolla *et al.* 2010).

Table 8 Sensitivity analysis of the inputs using Garson's algorithm

Inputs	D_h		K_h		V_h	
	RI %	Rank	RI %	Rank	RI %	Rank
H	12.94	3	9.43	4	6.35	4
S	13.32	2	9.89	3	14.32	2
Vs	6.15	5	5.54	5	1.81	6
PGA	7.11	4	12.45	2	8.34	3
G	4.60	6	5.19	6	3.79	5
SRS	55.73	1	55.55	1	65.5	1

*All six parameters of SRS are being treated as one to rank easily. SRS has more Relative Importance (RI) when treated individually as well. RI values are approximated.

6. Conclusions

The primary objective of the paper is to stress the importance of seismic structural safety of systems designed for wind. The authors applied computer-aided techniques such as machine learning to assess the design of NB structures classifying them into the wind and seismic models. Secondly, by analyzing the response features, the framework showed the importance of dynamic interaction of structures and model classification into coupled and uncoupled models as per the seismic demands. Lastly, using the proposed framework, the seismic responses of the structures are predicted. All of the objectives are successfully achieved in the current study with the development of an advanced computer-aided machine learning framework to classify the structures and to predict the seismic responses of NBs as well. The framework provides information about the design type (wind or seismic), design category (coupled or uncoupled) and seismic responses (K_h, V_h, D_h) of the structure. The framework is generalized by a significant variation in structure type, height, and ground motion parameters. The key outcomes of the study are summarized as below:

- The structures designed for wind must also be cross checked for the seismic safety.
- Analysis of different earthquakes and structures show that the seismic response of a system is different for the same EQ based on the dynamic interaction of the structures.
- It is demonstrated that based on the ground motion type, care should be taken while selecting the design model as coupled or uncoupled because for some earthquakes the coupled design is conservative and for others uncoupled design has a higher value of the engineering demand parameters.
- Among the ML classification techniques ENSEMBLE, KNN, SVM, and neural networks, the ENSEMBLE-1 model with a few modifications in the hyper-parameters, categorized the system into wind design, EQ coupled design and EQ uncoupled design with a TPR and accuracy of more than 90% and above.
- A seismic structure design assessment ratio A_c is introduced which can distinguish whether wind design, coupled EQ design, or uncoupled EQ design is required based on the earthquake response of the structure.
- Results show that the framework predicts the seismic responses K_h, V_h, D_h with reasonable accuracy of 90% to 96%. Among the different number of layers, neurons functions, algorithms, and transfer functions, 15 neurons and 1 hidden layer with Feed-forward back-propagation algorithm, TRAINLM as training function, and TANSIG as transfer function showed the most accurate results.
- The comparison of MISO and MIMO models demonstrated that the MISO model has more accuracy with a smaller number of neurons. The optimized number of neurons was 15 and 25 for both models respectively.
- Sensitivity analysis of the input parameters using Garson's algorithm has shown that response spectrum and interaction parameters are the most important for the seismic responses followed by the height parameter. Whereas the ground type and shear wave velocity have lower relative importance.

Although the results of this study are based on NBs, however, the concept can be extended to all types of structures in general. The database of the framework can be updated with several different parameters including different structure types and earthquakes.

Acknowledgement

This work is supported by the Korea Agency for Infrastructure Technology Advancement (KAIA) grant funded by the Ministry of Land, Infrastructure and Transport (Grant 22CTAP-C164093-02).

References

Abdel-Qader, I., Pashaie-Rad, S., Abudayyeh, O. and Yehia, S. (2006), "PCA-based algorithm for unsupervised bridge crack detection", *Adv. Eng. Softw.*, **37**(12), 771-778. https://doi.org/10.1016/j.advengsoft.2006.06.002.

Amiri, G.G. and Rajabi, E. (2018), "Maximum damage prediction for regular reinforced concrete frames under consecutive earthquakes", *Earthq. Struct.*, **14**(2), 129-142. https://doi.org/10.12989/eas.2018.14.2.129.

Aswegan, K., Larsen, R., Klemencic, R., Hooper, J. and Hasselbauer, J. (2017), "Performance-based wind and seismic engineering: benefits of considering multiple hazards", *Structures Congress 2017*, April.

Basaran, H., Demir, A., Ercan, E., Nohutcu, H., Hokelekli, E. and Kozanoglu, C. (2016), "Investigation of seismic safety of a masonry minaret using its dynamic characteristics", *Earthq. Struct.*, **10**(3), 523-538. http://doi.org/10.12989/eas.2016.10.3.523.

Bose, R.K. (2010), *Energy Efficient Cities: Assessment Tools and Benchmarking Practices*, World Bank Publications.

Bramer, M. (2013), "Ensemble classification", *Principles of Data Mining*, Springer, London.

Chen, E. (2012), "Multi-hazard design of mid-to high-rise structures", M.S. Thesis, University of Illinois at Urbana-Champaign, Urbana.

Chen, S.R. and Cai, C.S. (2004), "Accident assessment of vehicles on long-span bridges in windy environments", *J. Wind Eng. Indus. Aerodyn.*, **92**(12), 991-1024.

https://doi.org/10.1016/j.jweia.2004.06.002.
Choi, J.G. and Lee, C.Y. (2018), "An empirical study of soundproof wall with reduced wind load", *J. Korea Acad. Indus. Coop. Soc.*, **19**(12), 272-278. https://doi.org/10.5762/KAIS.2018.19.12.272.
City, B.L. and Assessment, E. (2010), "Urbanization and health", *Bull. World Hlth. Organ.*, **88**(4), 245-6.
Clairbois, J.P. and Garai, M. (2015), "The European standards for roads and railways noise barriers: State of the art 2015", *Proceedings of the 10th European Congress and Exposition on Noise Control Engineering: EuroNoise*, 45-50.
Code of Practice Noise Attenuation Walls.
Cortes, C. and Vapnik, V. (1995), "Support-vector networks", *Mach. Learn.*, **20**(3), 273-297. https://doi.org/10.1007/BF00994018.
Das, S.K. (2013), "10 Artificial neural networks in geotechnical engineering: modeling and application issues", *Metaheur. Water Geotech Transp. Eng.*, **45**, 231-267.
Deng, J., Gu, D., Li, X. and Yue, Z.Q. (2005), "Structural reliability analysis for implicit performance functions using artificial neural network", *Struct. Saf.*, **27**(1), 25-48. https://doi.org/10.1016/j.strusafe.2004.03.004.
Dhiman, N.K., Singh, B., Saini, P.K. and Garg, N. (2021), "Design of optimal noise barrier for metropolitan cities using artificial neural networks", *Optimization Methods in Engineering*, Springer, Singapore.
Do Kim, S. and Jung, W.Y. (2017), "Wind fragility for soundproof wall with the variation of section shape of frame", *Int. J. Civil Environ. Eng.*, **11**(11), 1551-1557.
Duru, E. (2016), "The design of an aluminium jam of noise barriers along (motor) ways".
Elmolla, E.S., Chaudhuri, M. and Eltoukhy, M.M. (2010), "The use of artificial neural network (ANN) for modeling of COD removal from antibiotic aqueous solution by the Fenton process", *J. Hazard. Mater.*, **179**(1-3), 127-134. https://doi.org/10.1016/j.jhazmat.2010.02.068.
Falcone, R., Lima, C. and Martinelli, E. (2020), "Soft computing techniques in structural and earthquake engineering: A literature review", *Eng. Struct.*, **207**, 110269. https://doi.org/10.1016/j.engstruct.2020.110269.
Farfani, H.A., Behnamfar, F. and Fathollahi, A. (2015), "Dynamic analysis of soil-structure interaction using the neural networks and the support vector machines", *Exp. Syst. Appl.*, **42**(22), 8971-8981. https://doi.org/10.1016/j.eswa.2015.07.053.
Fletcher, R. (2013), *Practical Methods of Optimization*, John Wiley & Sons.
Garson, D.G. (1991), "Interpreting neural network connection weights".
Gep, B. and Tiao, G.C. (1973), *Bayesian Inference in Statistical Analysis*, Addison-Wesley, Reading.
Gevrey, M., Dimopoulos, I. and Lek, S. (2003), "Review and comparison of methods to study the contribution of variables in artificial neural network models", *Ecol. Model.*, **160**(3), 249-264. https://doi.org/10.1016/S0304-3800(02)00257-0.
Grubeša, S., Domitrović, H. and Jambrošić, K. (2011), "Performance of traffic noise barriers with varying cross-section", *Promet-Traff. Transp.*, **23**(3), 161-168. https://doi.org/10.7307/ptt.v23i3.119.
Ham, H., Kim, T.J. and Boyce, D. (2005), "Assessment of economic impacts from unexpected events with an interregional commodity flow and multimodal transportation network model", *Transp. Res. Part A Policy Pract.*, **39**(10), 849-860. https://doi.org/10.1016/j.tra.2005.02.006.
Kappos, A.J. and Panagopoulos, G. (2004), "Performance-based seismic design of 3D R/C buildings using inelastic static and dynamic analysis procedures", *ISET J. Earthq. Technol.*, **41**(1), 141-158.
Kazama, M. and Noda, T. (2012), "Damage statistics (Summary of the 2011 off the Pacific Coast of Tohoku earthquake damage)", *Soil. Found.*, **52**(5), 780-792. https://doi.org/10.1016/j.sandf.2012.11.003.
Kiani, J., Camp, C. and Pezeshk, S. (2019), "On the application of machine learning techniques to derive seismic fragility curves", *Comput. Struct.*, **218**, 108-122. https://doi.org/10.1016/j.compstruc.2019.03.004.
Kim, H. and Roschke, P.N. (2006), "Fuzzy control of base-isolation system using multi-objective genetic algorithm", *Comput. Aid. Civil Infrastr. Eng.*, **21**(6), 436-449. https://doi.org/10.1111/j.1467-8667.2006.00448.x.
Kim, T., Kwon, O.S. and Song, J. (2019), "Response prediction of nonlinear hysteretic systems by deep neural networks", *Neur. Network.*, **111**, 1-10. https://doi.org/10.1016/j.neunet.2018.12.005.
Klingner, R.E., McNerney, M.T. and Busch-Vishniac, I.J. (2003), "Design guide for highway noise barriers", Research Report No. 1471-1474, Center for Transportation Research, Bureau of Engineering Research, University of Texas at Austin, Austin, TX, USA.
Knauer, H.S., Pedersen, S., Lee, C.S.Y. and Fleming, G.G. (2000), *FHWA Highway Noise Barrier Design Handbook*.
Kwon, S.D., Kim, D.H., Lee, S.H. and Song, H.S. (2011), "Design criteria of wind barriers for traffic. Part 1: Wind barrier performance", *Wind Struct.*, **14**(1), 55-70. https://doi.org/10.12989/was.2011.14.1.055.
Lagaros, N.D. and Papadrakakis, M. (2012), "Neural network based prediction schemes of the non-linear seismic response of 3D buildings", *Adv. Eng. Softw.*, **44**(1), 92-115. https://doi.org/10.1016/j.advengsoft.2011.05.033.
Lee, H.S. and Jeong, K.H. (2018), "Performance-based earthquake engineering in a lower-seismicity region: South Korea", *Earthq. Struct.*, **15**(1), 45-65. https://doi.org/10.12989/eas.2018.15.1.045.
León, J.X., Muñoz, W.A.P., Anaya, M., Vitola, J. and Tibaduiza, D.A. (2019), "Structural damage classification using machine learning algorithms and performance measures", *Structural Health Monitoring 2019.*
Li, S., Wang, Z., Guo, H. and Li, X. (2020), "Seismic performance of high strength steel frames with variable eccentric braces based on PBSD method", *Earthq. Struct.*, **18**(5), 527-542. https://doi.org/10.12989/eas.2020.18.5.527.
Li, X., Li, X. and Su, Y. (2016), "A hybrid approach combining uniform design and support vector machine to probabilistic tunnel stability assessment", *Struct. Saf.*, **61**, 22-42. https://doi.org/10.1016/j.strusafe.2016.03.001.
Li, Y. (2016), "Structure checking computations of sound barrier design", *5th International Conference on Sustainable Energy and Environment Engineering (ICSEEE 2016)*, Atlantis Press. https://doi.org/10.2991/icseee-16.2016.8.
Lin, J.L., Kuo, C.H., Chang, Y.W., Chao, S.H., Li, Y.A., Shen, W.C., ... & Hwang, S.J. (2020a), "Reconnaissance and learning after the February 6, 2018, earthquake in Hualien, Taiwan", *Bull. Earthq. Eng.*, **18**(10), 4725-4754. https://doi.org/10.1007/s10518-020-00878-0.
Lin, K.Y., Lin, T.K. and Lin, Y. (2020b), "Real-time seismic structural response prediction system based on support vector machine", *Earthq. Struct.*, **18**(2), 163-170. https://doi.org/10.12989/eas.2020.18.2.163.
Mangalathu, S. and Jeon, J.S. (2018), "Classification of failure mode and prediction of shear strength for reinforced concrete beam-column joints using machine learning techniques", *Eng. Struct.*, **160**, 85-94. https://doi.org/10.1016/j.engstruct.2018.01.008.
MathWorks, Inc. (2005), MATLAB: the Language of Technical Computing, Desktop Tools and Development Environment, Version 7, MathWorks.
MATLAB (2021), MATLAB.

McKenna, F. (2011), "OpenSees: a framework for earthquake engineering simulation", *Comput. Sci. Eng.*, **13**(4), 58-66. https://doi.org/10.1109/MCSE.2011.66.

McKenna, F., Mazzoni, S. and Fenves, G. (2011), "Open system for earthquake engineering simulation (OpenSees) software version 2.2.0", University of California, Berkeley, CA, USA.

Mirhosseini, R.T. (2017), "Seismic response of soil-structure interaction using the support vector regression", *Struct. Eng. Mech.*, **63**(1), 115-124. https://doi.org/10.12989/sem.2017.63.1.115.

Moeindarbari, H. and Taghikhany, T. (2018), "Seismic reliability assessment of base-isolated structures using artificial neural network: Operation failure of sensitive equipment", *Earthq. Struct.*, **14**(5), 425-436. https://doi.org/10.12989/eas.2018.14.5.425.

Neal, R.M. (1992), "Bayesian training of backpropagation networks by the hybrid Monte Carlo method", Technical Report CRG-TR-92-1, Dept. of Computer Science, University of Toronto, Canada.

Nguyen, D.T. (2006), *Finite Element Methods: Parallel-Sparse Statics and Eigen-Solutions*, Springer Science & Business Media.

Niewiadomski, L., Swierczyna, S. and Wuwer, W. (2014), "Capacity assessment and modification of high noise barriers", *Road. Bridges-Drogi i Mosty*, **13**(2), 145-155. https://doi.org/10.7409/rabdim.014.010.

Nusairat, J., Liang, R.Y., Engel, R., Hanneman, D., Abu-Hejleh, N. and Yang, K. (2004), "Drilled shaft design for sound barrier walls, signs, and signals", Report No. CDOT-DTD-R-2004, 8, Colorado Department of Transportation Research Branch.

Oh, B.K., Glisic, B., Park, S.W. and Park, H.S. (2020), "Neural network-based seismic response prediction model for building structures using artificial earthquakes", *J. Sound Vib.*, **468**, 115109. https://doi.org/10.1016/j.jsv.2019.115109.

Pan, Q. and Dias, D. (2017), "An efficient reliability method combining adaptive support vector machine and monte carlo simulation", *Struct. Saf.*, **67**, 85-95. https://doi.org/10.1016/j.strusafe.2017.04.006.

PEER Pacific Earthquake Engineering Research (PEER) Center, NGA Database. http://peer.berkeley.edu/nga/. Accessed 11 Oct 2021

Rajput, N. and Verma, S.K. (2014), "Back propagation feed forward neural network approach for speech recognition", *Proceedings of 3rd International Conference on Reliability, Infocom Technologies and Optimization*. IEEE, pp 1-6

Ryall, J. (2020), "Could a major earthquake soon strike South Korea?", DW Made for Minds.

Sainct, R., Feau, C., Martinez, J.M. and Garnier, J. (2020), "Efficient methodology for seismic fragility curves estimation by active learning on Support Vector Machines", *Struct. Saf.*, **86**, 101972. https://doi.org/10.1016/j.strusafe.2020.101972.

Salehi, H. and Burgueño, R. (2018), "Emerging artificial intelligence methods in structural engineering", *Eng. Struct.*, **171**, 170-189. https://doi.org/10.1016/j.engstruct.2018.05.084.

Salgado, R.A. and Guner, S. (2018), "A comparative study on nonlinear models for performance-based earthquake engineering", *Eng. Struct.*, **172**, 382-391. https://doi.org/10.1016/j.engstruct.2018.06.034.

Sim, V., Kim, S. and Jung, W. (2018), "Wind fragility for sign structure in Korea with chemical anchor connection", *MATEC Web of Conferences*, **186**, 02008.

Simpson, M.A. (1976), *Noise Barrier Design Handbook*, (No. FHWA-RD-76-58), Department of Transportation, USA.

Singh, T.N., Kanchan, R., Verma, A.K. and Saigal, K. (2005), "A comparative study of ANN and neuro-fuzzy for the prediction of dynamic constant of rockmass", *J. Earth Syst. Sci.*, **114**(1), 75-86. https://doi.org/10.1007/BF02702010.

Sonmez, H., Gokceoglu, C., Nefeslioglu, H.A. and Kayabasi, A. (2006), "Estimation of rock modulus: For intact rocks with an artificial neural network and for rock masses with a new empirical equation", *Int. J. Rock Mech. Min. Sci.*, **43**(2), 224-235. https://doi.org/10.1016/j.ijrmms.2005.06.007.

Suhanek, M., Djurek, I. and Petošić, A. (2021), "Combination of boundary element method and genetic algorithm for optimization of T-shape noise barrier", *Tehnički Vjesnik*, **28**(1), 77-81. https://doi.org/10.17559/TV-20190930132137.

Sun, Y., Xu, Y., Wang, X. and Zhu, H. (2020), "Experimental studies on column foot connections of novel fully enclosed noise barriers", *J. Constr. Steel Res.*, **172**, 106179. https://doi.org/10.1016/j.jcsr.2020.106179.

Tokunaga, M., Sogabe, M., Santo, T. and Ono, K. (2016a), "Dynamic response evaluation of tall noise barrier on high speed railway structures", *J. Sound Vib.*, **366**, 293-308. https://doi.org/10.1016/j.jsv.2015.12.015.

Tokunaga, M., Sogabe, M., Watanabe, T. and Tamai, S. (2016b), 土木学会. 構造工学論文集 62.

Tokunaga, M., Sogabe, M., Watanabe, T., Santo, T. and Tamai, S. (2013), "Dynamic response characteristics of the tall noise barrier on railway structures during seismicity", Proceedings of the Thirteenth East Asia-Pacific *Conference on Structural Engineering and Construction (EASEC-13)*, Sapporo, Japan, September.

Toledo, R., Aznárez, J.J., Maeso, O. and Greiner, D. (2015), "Optimization of thin noise barrier designs using evolutionary algorithms and a dual BEM formulation", *J. Sound Vib.*, **334**, 219-238. https://doi.org/10.1016/j.jsv.2014.08.032.

Turkeli, E., Karaca, Z. and Ozturk, H.T. (2017), "On the wind and earthquake response of reinforced concrete chimneys", *Earthq. Struct.*, **12**(5), 559-567. https://doi.org/10.12989/eas.2017.12.5.559.

Wassef, W.G., John, P.E., Kulicki, M., Withiam, J.L., Voytko, P.E.E.P., D'appolonia, P. and Mertz, D. (2010), "Application of AASHTO LRFD specifications to design of sound barriers".

Wen, Z.P., Chau, K.T. and Hu, Y.X. (2002), "Seismic fragility curves for wind designed-buildings in Hong Kong", Eds. Anson, M., Ko, J.M., Lam, E.S.S., *Advances in Building Technology*, Elsevier, Oxford.

Xu, J., Spencer Jr. B.F., Lu, X., Chen, X. and Lu, L. (2017), "Optimization of structures subject to stochastic dynamic loading", *Comput. Aid. Civil Infrastr. Eng.*, **32**(8), 657-673. https://doi.org/10.1111/mice.12274.

Zannin, P.H.T., do Nascimento, E.O., da Paz, E.C. and do Valle, F. (2018), "Application of artificial neural networks for noise barrier optimization", *Environ.*, **5**(12), 1-20. https://doi.org/10.3390/environments5120135.

Zheng, J., Li, Q., Li, X. and Luo, Y. (2020), "Train-induced fluctuating pressure and resultant dynamic response of semi enclosed sound barriers", *Shock Vib.*, **2020**, Article ID 6901564, https://doi.org/10.1155/2020/6901564.

DL

Notations

ANN	: Artificial Neural Network
D	: Maximum Displacement
D_1	: Displacement Limit
D_c	: Coupled Maximum Displacement
D_h	: Maximum Displacement Ratio
D_{uc}	: Uncoupled Maximum Displacement
E	: Elastic Modulus
EC	: Earthquake Coupled
EDP	: Engineering Demand Parameter
ELFP	: Equivalent Lateral Force Procedure

EQ : Earthquake
EUC : Earthquake Uncoupled
f_c' : Concrete Compressive Strength
FNR : False Negative Rate
F_y : Steel Yield Strength
G : Ground Type
H : Height of the Structure
I_z : 2nd Moment of Area
K_h : Maximum Acceleration Ratio
K_{hc} : Coupled Model Acceleration Ratio
K_{huc} : Uncoupled Model Acceleration Ratio
KNN : K-Nearest Neighbours
MIMO : Multi Input Multi Output
MISO : Multi Input Single Output
ML : Machine Learning
MSE : Mean Squared Error
M_w : Magnitude
NB : Noise Barrier
NLTHA : Non Linear Time History Analysis
PBSD : Performance Based Seismic Design
PGA : Peak Ground Acceleration
R : Linear Correlation Factor
RI : Relative Importance
S : Interaction Indicator
SDOF : Single Degree of Freedom
S_h : Design Category Ratio
SPSI : Soil Pile Strucutre Interaction
SRS : Short Response Spectrum
SSI : Soil Structure Interaction
SVM : Support Vector Machine
TARINBR : Bayesian Regularization
TPR : True Postive Rate
TRAINLM : Levenberg-Marquardt
TRAINSCG : Scaled Conjugate Gradient
V_h : Maximum Base Shear Ratio
V_s : Shear Wave Velocity
W : Wind